ACS APPLIED MATERIALS & INTERFACES

www.acsami.org

Research Article

Supramolecular Assembly of Shape Memory and Actuating Hydrogels for Programmable Shape Transformation

Jie Zhuo, Baoyi Wu, Jiawei Zhang,* Yu Peng, Huanhuan Lu, Xiaoxia Le, Shuxin Wei, and Tao Chen*

Cite This: *ACS Appl. Mater. Interfaces* 2022, 14, 3551−3558

Read Online

ACCESS | Metrics & More | Article Recommendations | Supporting Information

ABSTRACT: The deformable diversity of organisms in nature has inspired the development of bionic hydrogel actuators. However, the anisotropic structures of hydrogel actuators cannot be altered after the fabrication process, which restricts hydrogel actuators to provide complex and diverse shape deformations. Herein, we propose a dual programming method to generate numerous anisotropic structures from initial isotropic gelatin-containing hydrogels; the isotropic hydrogel blocks could be first assembled into anisotropic structures based on the coil-triple helix transition of gelatin, and then, the assembled hydrogels could further be fixed into various temporary anisotropies, so that they can produce complex and diverse deformations under the stimulation of pH. In addition, the shape programming and deformation behaviors are reversible. This dual programming method provides more potential for the application of hydrogel actuators in soft robots and bionics.

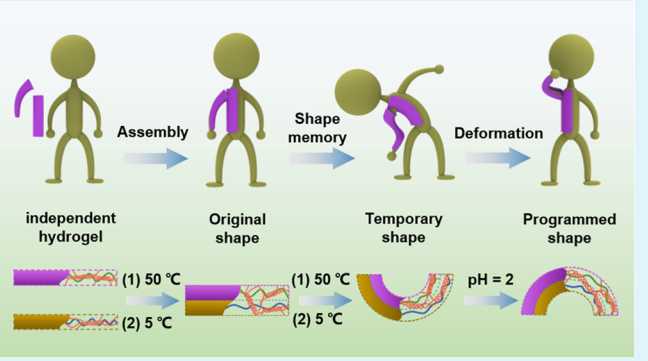

KEYWORDS: *dual programming method, supramolecular assembly, shape memory, deformation of hydrogel, soft hydrogel robot*

1. INTRODUCTION

The biodiversity of nature provides a lot of inspiration for the development of artificial intelligent materials.[1−6] Among which, polymeric hydrogel actuators could produce reversible biomimetic shape transformations;[7−9] moreover, they are high water content, are as soft as living tissues, and could have good biocompatibility, and therefore, they have shown significant potential in the fields of soft robotics[10,11] and information storage.[12,13] In the past decades, hydrogel actuators have been able to achieve simple bending, folding, and complex deformation behaviors through the construction of bilayer,[14,15] gradient,[16−20] patterned,[21,22] or other anisotropic structures.[23,24] In order to further manipulate the anisotropic structures of hydrogel actuators, temporary anisotropy has been developed. For example, Liu et al. have introduced transient structural anisotropy into hydrogels of *N*-isopropylacrylamide and stearyl acrylate, which could produce programmable thermoresponsive shape transformations.[25] In our previous work, we have applied a shape memory strategy to construct temporary anisotropy on a bilayer hydrogel and have realized a variety of reversible complex deformations.[26] However, the initial structures of these hydrogel actuators are generally determined by the preparation process, and if the initial structures of the hydrogel actuators could also be adjusted after the construction, the subsequent deformation behaviors could be more diversified, which would expand the potential applications of hydrogel actuators.

In order to alter the initial structures of hydrogel actuators, another promising strategy, supramolecular assembly was considered because it could weld simple hydrogel blocks into complex structures.[27,28] A few hydrogel actuators have been fabricated by the supramolecular strategy. Xie et al. have utilized host−guest interactions to assemble hydrogel strips into three-dimensional hydrogel actuators.[29] We have applied dynamic boronic ester bonds to weld hydrogel blocks into smart actuators with complex deformations.[30] It could be anticipated that if supramolecular assembly and shape memory are employed as dual shape programming methods, compared with the traditional anisotropic structure hydrogels, the hydrogels with the dual programming method are able to make reversible and more diverse designs from the initial isotropic structures. Meanwhile, by combining assembly and shape memory, complex 3D-deformed hydrogels can be obtained.

Herein, we present a dual shape programming strategy in which assembly is used as the first programming and shape memory is used as the second programming. Polyacrylamide/gelatin (AG) hydrogels and poly (acrylamide-*co*-methacrylic

Received: November 12, 2021
Accepted: December 27, 2021
Published: January 5, 2022

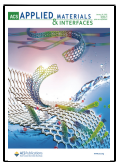

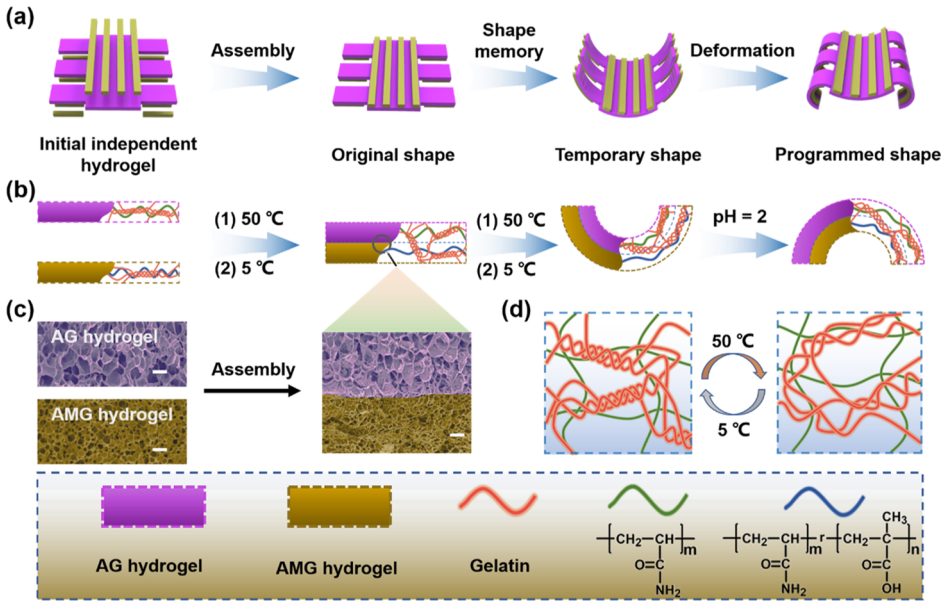

Figure 1. (a) Schematic illustration of formation of a crawler robot obtained through the welding and shape memory of the AG hydrogel and AMG hydrogel. (b) Schematic illustration of the mechanism of welding, shape memory, and actuating process. (c) SEM images of the AG hydrogel and AMG hydrogel and the cross section of the bilayer hydrogel. (d) Schematic illustration of the thermoresponsive coil-triple helix transition of gelatin. Scale bars: 10 μm.

acid)/gelatin (AMG) hydrogels were fabricated first, supramolecular assembly could be used as the first programming to control the initial anisotropy of hydrogels, and then, shape memory behavior is used as the second programming to generate temporary anisotropy (Figure 1a,b). Finally, a reptilian hydrogel can be obtained. A strong interface of AG and AMG hydrogels can be obtained by welding (Figure 1c) because of the thermoresponsive coil-triple helix transition of gelatin (Figure 1d). The synergistic effect of the two shape programming methods could accomplish diverse deformation behaviors from isotropic hydrogel blocks, which can greatly enrich the deformation results of actuators.

2. EXPERIMENTAL SECTION

2.1. Materials. Gelatin (≥99.5%), *N*,*N*′-methylene bis(acrylamide) (BIS, ≥99%), methylacrylic acid (MAA, ≥98%), *N*,*N*,*N*′,*N*′-tetramethyl ethylenediamine (TEMED, ≥99%), ammonium persulfate (APS, ≥98%), and rhodamine B (≥99.7%) were purchased from Aladdin Chemistry Co. Ltd. Acrylamide (AAm, ≥99.5%) and sodium hydroxide (NaOH, ≥99.7%) were purchased from Sinopharm Chemical Reagent Co. Ltd. All reagents were used as received.

2.2. Instruments. The lyophilizing process was conducted in the DGJ-10C freeze dryer (Shanghai Boden Biological Science and Technology Co. Ltd.). The hydrogel modules used for assembly were obtained by a laser cutter (GY-460 bought from Shandong Liaocheng Guangyue Laser Equipment Co., Ltd.). The microstructure of the hydrogel was analyzed by field-emission scanning electron (Hitachi S-4800) microscopy. The rheological measurement was performed on a stress-controlled rheometer (TA-dhr2) equipped with a geometry of 25 mm parallel plates. The tensile test was conducted on the Z1 Zwick/Roell Universal Testing System (Zwick).

2.3. Preparation of AG Hydrogel. 1.6 g of gelatin was dissolved in 8.4 mL of deionized water to get gelatin solution (16 wt %) at 60 °C. 0.7 g of AAm, 0.04 g of BIS, 0.04 g of APS, and 5 μL of TEMED were dissolved in the abovementioned solution. The solution was transferred into a 0.5 mm PDMS mold attached to a piece of glass. Then, the other piece of glass was covered on the solution under the condition of insulating air. The hydrogel was obtained after gelation for 12 h at 35 °C.

2.4. Preparation of AMG Hydrogel. 1.6 g of gelatin was dissolved in 8.4 mL of deionized water to get gelatin solution (16 wt %) at 60 °C. 0.3 g of AAm, 0.7 g of MAA, 0.328 g of NaOH, 0.04 g of BIS, 0.04 g of APS, and 10 μL of TEMED were dissolved in the abovementioned solution. The solution was added into a 0.5 mm PDMS mold attached to a piece of glass. Then, the other piece of glass was covered on the solution to insulating air. After gelation for 12 h at 35 °C, the AMG hydrogel was obtained.

2.5. Welding of AG Hydrogel and AMG Hydrogel. The AMG hydrogel was attached to the AG hydrogel. After heating for 10 min at 50 °C and cooling to room temperature, the bilayer hydrogel was obtained.

3. RESULTS AND DISCUSSION

The two semi-interpenetrating hydrogels were prepared by free radical polymerization of monomers in the presence of gelatin. Because of the coil-triple helix transition of gelatin induced by temperature,[31] two strips of AG and AMG hydrogels were pushed together at 50 °C, and they could merge together when the temperature was decreased to 20 °C due to the entanglement of gelatin chains at the interface. As shown in Figure S1, the AG layer and the AMG layer exhibit typical porous microstructures, and the two layers are joined tightly. In order to evaluate the connecting strength of the two layers, a bilayer hydrogel that is partially welded was stretched, and the fracture did not occur at the connecting area, reflecting a good welding strength (Figure S2). According to the peeling test, an AG hydrogel strip and an AMG hydrogel strip were prepared. Also, half of the two hydrogel strips were assembled, while the other half were not. Then, one layer of hydrogel was fixed at the bottom of the Universal Testing System, and the other side of the unassembled end was clipped on the Universal Testing System to peel it off. The bilayer hydrogel shows an interfacial peeling force of about 120 N/m, indicating that the two layers are bonded stably (Figure 2a). Moreover, according to the tensile experiment, the AMG hydrogel exhibits a larger elongation at break and a smaller maximum tensile stress compared with the AG hydrogel, and the bilayer hydrogel shows

https://doi.org/10.1021/acsami.1c21941
ACS Appl. Mater. Interfaces 2022, 14, 3551−3558

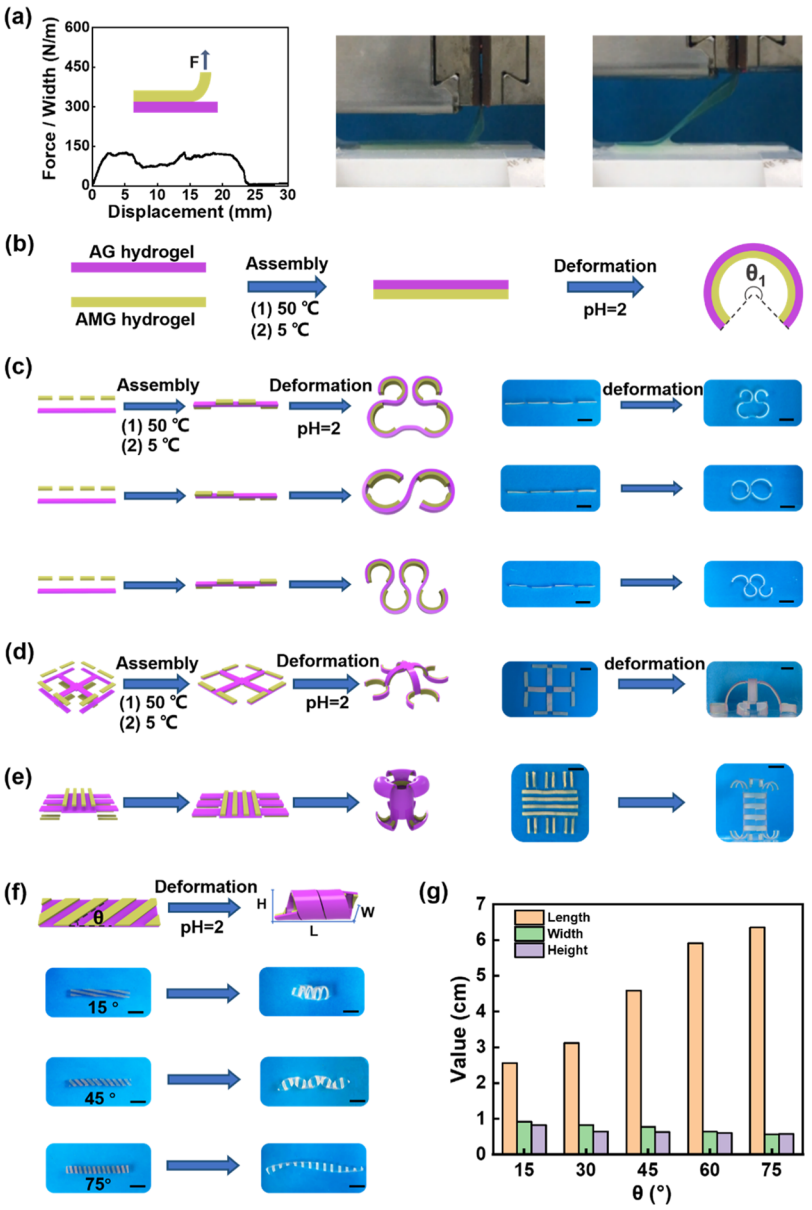

Figure 2. (a) Curves of the peeling force per width of the hydrogel sheet versus displacement for interface bonding and photographs of the peeling process. (b) Schematic illustration of the process of welding and deformation of an AG hydrogel strip and an AMG hydrogel strip. (c) Anisotropic structures constructed by AG hydrogel strips and AMG hydrogel strips and the further deformation behaviors. (d) Assembly of AG and AMG hydrogel strips deforming into a standing grab structure. (e) Assembly of AG and AMG hydrogels deforming into a lantern structure. (f) Different deformation behaviors caused by sloping distribution in different degrees of AMG hydrogel strips on an AG hydrogel sheet. (g) Relationship between the length, width, and height of helical structures and the inclination angle of AMG hydrogel strips. Scale bars: 1 cm.

neutralized tensile properties with an elongation at break exceeding 200% (Figures S3 and S4).

Because the equilibrium swelling ratios of the AMG hydrogel increase with the increasing pH value due to the existence of carboxylic acid groups (Figure S5), the AG/AMG bilayer hydrogel could deform upon the trigger of pH (Figure 2b). It is well known that the shape transformation behaviors of hydrogel actuators are essentially determined by their anisotropic structures. As shown in Figure 2c, one long AG hydrogel strip is assembled with four short AMG hydrogel strips and three different anisotropic structures could be achieved through changing the distribution of short hydrogel strips on long hydrogel strips, leading to three different actuating performances. Furthermore, abundant patterned structures could be obtained by welding. The cross-shaped structure is assembled from hydrogel strip arches in the middle and forms four grippers under the condition of pH 2 (Figure 2d). The two-dimensional structure assembled from hydrogel strips and sheets could deform into a three-dimensional lantern (Figure 2e). Moreover, for the assembly of hydrogel sheets and hydrogel strips, the deformation behaviors can be controlled by changing the distribution angle of the AMG hydrogel strips on the AG hydrogel sheets. When the angle between the stripe and the plane increases from 15 to 75°, the deformation results of the hydrogel also vary greatly (Figure 2f). As the angle increases, the length of the helix formed by the deformation of the hydrogel sheets increases and the height and width of the helix slightly become smaller (Figure 2g). It should be noted that the assembly process is reversible. As shown in Figure S6, the ends of an AMG hydrogel strip and an AG hydrogel strip are welded

https://doi.org/10.1021/acsami.1c21941
ACS Appl. Mater. Interfaces 2022, 14, 3551−3558

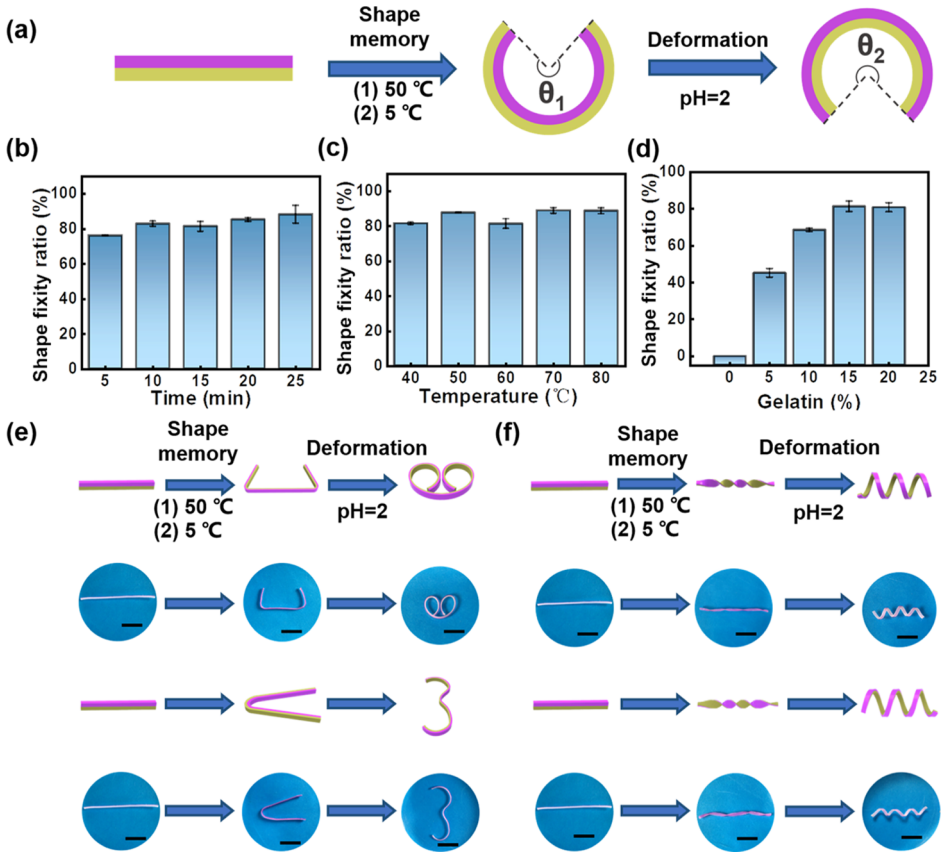

Figure 3. (a) Schematic illustration of the process of shape memory and deformation of an AG−AMG bilayer hydrogel strip. (b) Variation of shape fixity ratios, as the shape memory time is from 5 to 25 min. (c) Variation of shape fixity ratios, as the shape memory temperature is from 40 to 80 °C. (d) Variation of shape fixity ratios, as the mass fraction of gelatin in gelatin solution is from 0 to 15%. (e) Deformation of bilayer hydrogel strips after shape fixation. (f) Deformation of bilayer hydrogel strips after shape fixation into twist to the right or left. Scale bars: 1 cm.

together. Because of the difference of the swelling ratio between the two hydrogel strips, the bilayer hydrogel will deform into the shape of an arch bridge. Under the condition of 50 °C and pH 12, the bilayer hydrogel can restore the initial shape and disassembly. Then, the two hydrogel strips can be assembled into a bilayer hydrogel and deform into a semicircle under acidic conditions.

Because both the AG hydrogel and the AMG hydrogel contain gelatin, the AG-AMG bilayer hydrogel exhibits shape memory property due to single coil-triple helix transition of gelatin. The rheological results show that the storage modulus (G') and loss modulus (G'') of the AG hydrogel and AMG hydrogel at 50 °C are less than those at 20 °C (Figure S7), which indicates the melting of gelatin at relatively high temperature and gelation of gelatin at low temperature. When a bilayer hydrogel strip is manually deformed at 50 °C and then transferred to a cold environment (5 °C), the deformed shape could be fixed because of the random coil of gelatin would change to tripe helix at low temperature (Figure 3a). The shape fixity ratio is defined by the following equation

$$R_f = \frac{\theta_m}{\theta_d} \times 100\%$$

where θ_m and θ_d are the bending angles of the deformed shape and memorized shape of hydrogels, respectively (Figure S8).

We have evaluated both the exogenous and endogenous factors that may affect the shape fixity ratio. As shown in Figure 3b, when the deformation temperature is set at 50 °C, the shape fixity ratio only shows a slight increment with the processing time increasing from 5 to 25 min, indicating that most of the gelatin chains inside the hydrogel would turn into the coil state when the hydrogel is placed at 50 °C, while when the processing time is set at 10 min, the temperature of shape deformation that varies from 40 to 80 °C has little effect on the shape fixity ratio (Figure 3c). However, the shape fixity ratio is highly dependent on the mass fraction of gelatin in gelatin solution. When the mass fraction of gelatin in gelatin solution increases from 0 to 15%, the shape fixity ratio of the hydrogel increases significantly and reaches the maximum value of 80% when the mass fraction of gelatin in gelatin solution is 15% (Figure 3d).

After shape fixation, the circular shape hydrogel would transform when the pH of environment decreases to 2 (Figure S9). If a hydrogel strip is bent for one or two times and then the deformed shapes were fixed, "3" or heart-shaped can be obtained when the hydrogel further actuates in the pH of 2 (Figure 3e). Moreover, if a hydrogel strip is programmed by left lateral torsion or right lateral torsion, the hydrogel strip can be further transformed from two dimensions (2D) to three dimensions (3D) to obtain the structures of the left helix and right helix (Figure 3f). It should be noted that the shape programming process is reversible, as shown in Figure S10; when a bilayer hydrogel strip is programed by shape fixation and deforms, it could restore to the original straight state under the condition of 50 °C and pH of 12, and it could be further memorized into another shape and actuates in pH 2.

https://doi.org/10.1021/acsami.1c21941
ACS Appl. Mater. Interfaces 2022, 14, 3551−3558

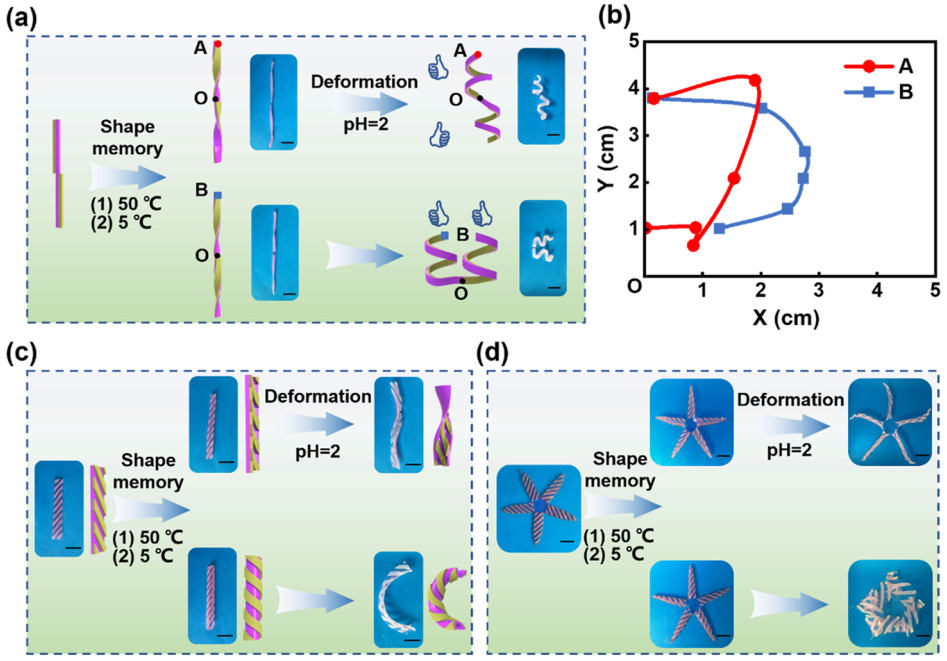

Figure 4. (a) Illustration and images showing the deformation of a sandwich-shaped hydrogel strip with different temporary shapes. (b) Motion track of the deformation process of the endpoints of hydrogels. (c) Illustration and images showing the shape fixation and deformation of the assembly of AG hydrogel sheets and AMG hydrogel strips. (d) Shape fixation and deformation behavior of star-shaped hydrogel assembly. Scale bars: 1 cm.

Therefore, shape memory could be regarded as the second shape programming strategy, and when combined with the first shape programming strategy welding, diverse shape transformation behaviors could be achieved. For example, under the premise that a hydrogel strip is fixed into the torsion structure through shape memory first and the helical structure could be obtained by the further shape transformation of the hydrogel strip, a multihelix coexistence structure can be obtained by combining shape memory behavior and welding functions. As shown in Figure 4a, an AG hydrogel strip is first programmed by attaching one AMG hydrogel strip on both sides in a central symmetrical way; after the second shape programming, the hydrogel can produce two temporary structures. The first one is the upper and lower parts both twisted to the same direction, and the second is the upper and lower parts belong to different directions. When the upper part is twisted to the right and the lower part is twisted to the left, the hydrogel would transform into a structure with a right helix plus a left helix. When the upper part and the lower part are both twisted to the right, the deformation result is two right helix structures.

Furthermore, the motion track of the deformation process from the temporary anisotropy is described in detail. As shown in Figure 4b, taking the symmetry center O of the hydrogel as a reference point to establish the plane right-angle coordinate system, the horizontal distance between point A and point O is recorded as X and the vertical distance is recorded as Y. In this way, the trajectories of the hydrogel ends A and B are described. When the twist direction of the upper part and the lower part is opposite, due to the cancellation of the internal stress in the horizontal direction, point A is less deviated from the *Y* axis in the motion process, and it is still on the *Y* axis after the deformation is complete. On the contrary, when the twist direction of the upper part and the lower part is the same, due to the increase of the internal stress in the horizontal direction, point B is more deviated from the *Y* axis in the motion process, and it is far away from the *Y* axis when the deformation is complete (Figure 4b).

In addition to the programmable deformations of strips and sheets, hydrogel strips and hydrogel sheets could also be programmed to achieve a complex shape deformation. As shown in Figure 4c, hydrogel strips are welded to a rectangular hydrogel sheet at a 45° angle, and then, the assembled hydrogel sheet is fixed into a concave or convex shape. When the hydrogel is programmed in a concave shape by shape memory, the stress in the horizontal direction is increased, resulting in a helix shape. On the contrary, when the hydrogel is fixed in a convex shape, the stress in the horizontal direction is reduced or even offset and the hydrogel would turn into an arch shape. In addition, a hydrogel flower is prepared by assembled hydrogel strips on the petals at an angle of 45°, if all the petals are fixed in a concave shape, the hydrogel can deform into a star shape. If all the petals are fixed in the convex shape, the petals would bent inward, and the hydrogel can deform into a pentagon (Figure 4d). In order to explore the effect of shape memory on the deformation of hydrogels, the deformation results of the asymmetric triangular hydrogel and hexagonal triangular hydrogel before and after shape memory are compared. It can be seen that the deformation results of hydrogels after shape memory vary greatly compared with that before shape memory, which further indicates that the second programming can be used to adjust the deformation results of hydrogels (Figures S11 and S12).

The dual programming shape deformation behaviors encourage us to investigate the biomimetic shape deformation behaviors. As shown in Figure 5a, a soft robot is prepared by the AMG hydrogel and it cannot deform because of the isotropic structures. When the first programming is introduced, any part of the soft robot can be welded to form the corresponding anisotropic structure and produce the expected deformation. For example, to imitate the process of raising an arm of the human body, an AG hydrogel strip is welded to the arm of the soft robot to construct an anisotropic structure. The arm of the

https://doi.org/10.1021/acsami.1c21941
ACS Appl. Mater. Interfaces 2022, 14, 3551−3558

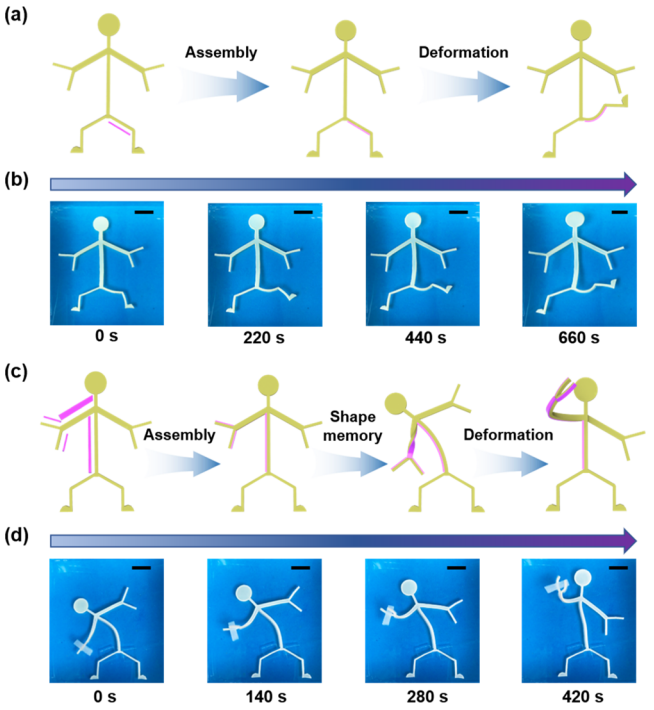

Figure 5. (a) Illustration and (b) digital photographs of the assembly and leg lifting of a hydrogel robot. (c) Illustration and (d) digital photographs of the assembly, clamping the object, raising the waist, and lifting the object to the front of a hydrogel robot. Scale bars: 1 cm.

hydrogel robot can bend in the pH of 2 due to the different swelling ratios between the AG hydrogel and the AMG hydrogel (Figure S13, Movie S1). Similarly, an AG hydrogel strip is welded to the leg of the hydrogel robot (Figure 5a), and the leg of the soft robot can gradually lift up to achieve the kick action in the pH of 2 (Figure 5b, Movie S2). In order to further imitate the complex movements of the human body, the two programming methods of welding and shape memory are combined. To simulate a person bend down to pick up an object on the ground and lift it up, first of all, AG hydrogels are welded on the outside of the fingers, arms, and waist of the hydrogel robot to construct anisotropic structures. Then, torsion is introduced into the arm, and bending is provided to the body of the soft robot as the secondary programming (Figure 5c, Movie S3). After shape memory, the arm of the soft robot is fixed into a spiral shape and can produce relative motion with the body in the pH of 2 to simulate the twisting process of the human arm joint. Therefore, after welding the corresponding parts and fixing the arm in a torsion shape and the body in a bend posture, the soft robot can realize the continuous movement of clamping the object, raising the waist, and lifting the object to the front under the synergistic action of fingers, arms, and waist (Figure 5d).

4. CONCLUSIONS

In conclusion, a new strategy of dual programming has been proposed to achieve complex deformation of hydrogels. Using the reversible coil-triple helix transition of gelatin chains, two gelatin-containing hydrogels could be assembled, which could be regarded as the first programming method to modify the initial anisotropy of hydrogels, and then, shape memory is used as the second programming method to generate temporary anisotropy. Therefore, various anisotropic structures could be achieved starting from several isotropic hydrogel blocks, leading to diverse complex shape transformation behaviors. Based on the synergy of shape memory and welding, multiple parts of the soft robot could move synchronously to simulate the complex and coherent in situ motion of the human body. We believe that our strategy to achieve programmable complex deformation could provide innovative ideas for the design of biomimetic hydrogel actuators.

■ ASSOCIATED CONTENT

Supporting Information

The Supporting Information is available free of charge at https://pubs.acs.org/doi/10.1021/acsami.1c21941.

SEM images of hydrogels, digital photographs of a bilayer hydrogel during stretching, stress−strain curves of hydrogels, dynamic oscillatory frequency sweeps of hydrogels, schematic illustration of the shape memory process, variation of the bending angle of a hydrogel strip as a function of time, digital photographs of repeated shape memory-deformation behavior, digital photographs of the deformation of a triangular hydrogel and a snowflake-shaped hydrogel, and illustration and digital photographs of hand raising of a hydrogel robot (PDF)

Bending of the arm of the hydrogel robot in the pH of 2 (MP4)

Lifting up of the leg of the soft robot to achieve the kick action in the pH of 2 (MP4)

Introduction of torsion to the arm and bending to the body of the soft robot as the secondary programming (MP4)

■ AUTHOR INFORMATION

Corresponding Authors

Jiawei Zhang − *Key Laboratory of Marine Materials and Related Technologies, Zhejiang Key Laboratory of Marine Materials and Protective Technologies, Ningbo Institute of Materials Technology and Engineering, Chinese Academy of Sciences, Ningbo 315201, China; School of Chemical Sciences, University of Chinese Academy of Sciences, Beijing 100049, China;* orcid.org/0000-0002-3182-9239; Email: zhangjiawei@nimte.ac.cn

Tao Chen − *Key Laboratory of Marine Materials and Related Technologies, Zhejiang Key Laboratory of Marine Materials and Protective Technologies, Ningbo Institute of Materials Technology and Engineering, Chinese Academy of Sciences, Ningbo 315201, China; School of Chemical Sciences, University of Chinese Academy of Sciences, Beijing 100049, China;* orcid.org/0000-0001-9704-9545; Email: tao.chen@nimte.ac.cn

Authors

Jie Zhuo − *Key Laboratory of Marine Materials and Related Technologies, Zhejiang Key Laboratory of Marine Materials and Protective Technologies, Ningbo Institute of Materials Technology and Engineering, Chinese Academy of Sciences, Ningbo 315201, China; School of Chemical Sciences, University of Chinese Academy of Sciences, Beijing 100049, China*

Baoyi Wu − *Key Laboratory of Marine Materials and Related Technologies, Zhejiang Key Laboratory of Marine Materials and Protective Technologies, Ningbo Institute of Materials Technology and Engineering, Chinese Academy of Sciences, Ningbo 315201, China; School of Chemical Sciences,*

https://doi.org/10.1021/acsami.1c21941
ACS Appl. Mater. Interfaces 2022, 14, 3551−3558

University of Chinese Academy of Sciences, Beijing 100049, China

Yu Peng − *Key Laboratory of Marine Materials and Related Technologies, Zhejiang Key Laboratory of Marine Materials and Protective Technologies, Ningbo Institute of Materials Technology and Engineering, Chinese Academy of Sciences, Ningbo 315201, China; School of Chemical Sciences, University of Chinese Academy of Sciences, Beijing 100049, China*

Huanhuan Lu − *Key Laboratory of Marine Materials and Related Technologies, Zhejiang Key Laboratory of Marine Materials and Protective Technologies, Ningbo Institute of Materials Technology and Engineering, Chinese Academy of Sciences, Ningbo 315201, China; School of Chemical Sciences, University of Chinese Academy of Sciences, Beijing 100049, China*

Xiaoxia Le − *Key Laboratory of Marine Materials and Related Technologies, Zhejiang Key Laboratory of Marine Materials and Protective Technologies, Ningbo Institute of Materials Technology and Engineering, Chinese Academy of Sciences, Ningbo 315201, China; School of Chemical Sciences, University of Chinese Academy of Sciences, Beijing 100049, China*

Shuxin Wei − *Key Laboratory of Marine Materials and Related Technologies, Zhejiang Key Laboratory of Marine Materials and Protective Technologies, Ningbo Institute of Materials Technology and Engineering, Chinese Academy of Sciences, Ningbo 315201, China; School of Chemical Sciences, University of Chinese Academy of Sciences, Beijing 100049, China*

Complete contact information is available at: https://pubs.acs.org/10.1021/acsami.1c21941

Notes

The authors declare no competing financial interest.

■ ACKNOWLEDGMENTS

This work was supported by National Key Research and Development Program of China (2018YFB1105100) and National Natural Science Foundation of China (51873223 and 52073295).

■ REFERENCES

(1) Kempaiah, R.; Nie, Z. From Nature to Synthetic Systems: Shape Transformation in Soft Materials. *J. Mater. Chem. B* **2014**, *2*, 2357−2368.

(2) Zhao, Z.; Fang, R.; Rong, Q.; Liu, M. Bioinspired Nanocomposite Hydrogels with Highly Ordered Structures. *Adv. Mater.* **2017**, *29*, 1703045.

(3) Ajdary, R.; Tardy, B. L.; Mattos, B. D.; Bai, L.; Rojas, O. J. Plant Nanomaterials and Inspiration from Nature: Water Interactions and Hierarchically Structured Hydrogels. *Adv. Mater.* **2021**, *33*, No. e2001085.

(4) Matsuda, T.; Kawakami, R.; Namba, R.; Nakajima, T.; Gong, J. P. Mechanoresponsive self-growing hydrogels inspired by muscle training. *Science* **2019**, *363*, 504−508.

(5) Shang, L.; Zhang, W.; Xu, K.; Zhao, Y. Bio-inspired intelligent structural color materials. *Mater. Horiz.* **2019**, *6*, 945−958.

(6) Ji, X.; Li, Z.; Hu, Y.; Xie, H.; Wu, W.; Song, F.; Liu, H.; Wang, J.; Jiang, M.; Lam, J. W. Y.; Zhong Tang, B. Bioinspired Hydrogels with Muscle-Like Structure for AIEgen-Guided Selective Self-Healing. *CCS Chem* **2021**, *3*, 1146−1156.

(7) Fan, W.; Shan, C.; Guo, H.; Sang, J.; Wang, R.; Zheng, R.; Sui, K.; Nie, Z. Dual-gradient Enabled Ultrafast Biomimetic Snapping of Hydrogel Materials. *Sci. Adv.* **2019**, *5*, No. eaav7174.

(8) Yuk, H.; Lin, S.; Ma, C.; Takaffoli, M.; Fang, N. X.; Zhao, X. Hydraulic Hydrogel Actuators and Robots Optically and Sonically Camouflaged in Water. *Nat. Commun.* **2017**, *8*, 14230.

(9) Cui, Y.; Li, D.; Gong, C.; Chang, C. Bioinspired Shape Memory Hydrogel Artificial Muscles Driven by Solvents. *ACS Nano* **2021**, *15*, 13712−13720.

(10) Zhao, Y.; Xuan, C.; Qian, X.; Alsaid, Y.; Hua, M.; Jin, L.; He, X. Soft phototactic swimmer based on self-sustained hydrogel oscillator. *Sci. Robot.* **2019**, *4*, No. eaax7112.

(11) Han, D.; Farino, C.; Yang, C.; Scott, T.; Browe, D.; Choi, W.; Freeman, J. W.; Lee, H. Soft Robotic Manipulation and Locomotion with a 3D Printed Electroactive Hydrogel. *ACS Appl. Mater. Interfaces* **2018**, *10*, 17512−17518.

(12) Le, X.-X.; Lu, W.; He, J.; Serpe, M. J.; Zhang, J.-W.; Chen, T. Ionoprinting controlled information storage of fluorescent hydrogel for hierarchical and multi-dimensional decryption. *Sci. China Mater.* **2018**, *62*, 831−839.

(13) Wu, B.; Lu, H.; Le, X.; Lu, W.; Zhang, J.; Théato, P.; Chen, T. Recent Progress in the Shape Deformation of Polymeric Hydrogels from Memory to Actuation. *Chem. Sci.* **2021**, *12*, 6472−6487.

(14) Ma, C.; Lu, W.; Yang, X.; He, J.; Le, X.; Wang, L.; Zhang, J.; Serpe, M. J.; Huang, Y.; Chen, T. Bioinspired Anisotropic Hydrogel Actuators with On-Off Switchable and Color-Tunable Fluorescence Behaviors. *Adv. Funct. Mater.* **2018**, *28*, 1704568.

(15) Zhao, H.; Huang, Y.; Lv, F.; Liu, L.; Gu, Q.; Wang, S. Biomimetic 4D-Printed Breathing Hydrogel Actuators by Nanothylakoid and Thermoresponsive Polymer Networks. *Adv. Funct. Mater.* **2021**, *31*, 2105544.

(16) Bi, Y.; Du, X.; He, P.; Wang, C.; Liu, C.; Guo, W. Smart Bilayer Polyacrylamide/DNA Hybrid Hydrogel Film Actuators Exhibiting Programmable Responsive and Reversible Macroscopic Shape Deformations. *Small* **2020**, *16*, No. e1906998.

(17) Zhao, L.; Huang, J.; Zhang, Y.; Wang, T.; Sun, W.; Tong, Z. Programmable and Bidirectional Bending of Soft Actuators Based on Janus Structure with Sticky Tough PAA-Clay Hydrogel. *ACS Appl. Mater. Interfaces* **2017**, *9*, 11866−11873.

(18) Zhao, Q.; Liang, Y.; Ren, L.; Yu, Z.; Zhang, Z.; Ren, L. Bionic intelligent hydrogel actuators with multimodal deformation and locomotion. *Nano Energy* **2018**, *51*, 621−631.

(19) Jiang, Z.; Tan, M. L.; Taheri, M.; Yan, Q.; Tsuzuki, T.; Gardiner, M. G.; Diggle, B.; Connal, L. A. Strong, Self-Healable, and Recyclable Visible-Light-Responsive Hydrogel Actuators. *Angew. Chem., Int. Ed. Engl.* **2020**, *59*, 7049−7056.

(20) Tan, Y.; Wang, D.; Xu, H.; Yang, Y.; Wang, X.-L.; Tian, F.; Xu, P.; An, W.; Zhao, X.; Xu, S. Rapid Recovery Hydrogel Actuators in Air with Bionic Large-Ranged Gradient Structure. *ACS Appl. Mater. Interfaces* **2018**, *10*, 40125−40131.

(21) Hao, X. P.; Xu, Z.; Li, C. Y.; Hong, W.; Zheng, Q.; Wu, Z. L. Kirigami-Design-Enabled Hydrogel Multimorphs with Application as a Multistate Switch. *Adv. Mater.* **2020**, *32*, No. e2000781.

(22) Peng, X.; Liu, T.; Zhang, Q.; Shang, C.; Bai, Q.-W.; Wang, H. Surface Patterning of Hydrogels for Programmable and Complex Shape Deformations by Ion Inkjet Printing. *Adv. Funct. Mater.* **2017**, *27*, 1701962.

(23) Gevorkian, A.; Morozova, S. M.; Kheiri, S.; Khuu, N.; Chen, H.; Young, E.; Yan, N.; Kumacheva, E. Actuation of Three-Dimensional-Printed Nanocolloidal Hydrogel with Structural Anisotropy. *Adv. Funct. Mater.* **2021**, *31*, 2010743.

(24) Qin, H.; Zhang, T.; Li, N.; Cong, H.-P.; Yu, S.-H. Anisotropic and Self-healing Hydrogels with Multi-responsive Actuating Capability. *Nat. Commun.* **2019**, *10*, 2202.

(25) Liu, K.; Zhang, Y.; Cao, H.; Liu, H.; Geng, Y.; Yuan, W.; Zhou, J.; Wu, Z. L.; Shan, G.; Bao, Y.; Zhao, Q.; Xie, T.; Pan, P. Programmable Reversible Shape Transformation of Hydrogels Based on Transient Structural Anisotropy. *Adv. Mater.* **2020**, *32*, No. e2001693.

(26) Lu, H.; Wu, B.; Yang, X.; Zhang, J.; Jian, Y.; Yan, H.; Zhang, D.; Xue, Q.; Chen, T. Actuating Supramolecular Shape Memorized Hydrogel Toward Programmable Shape Deformation. *Small* **2020**, *16*, 2005461.
(27) Wang, Q.; Liu, Z.; Tang, C.; Sun, H.; Zhu, L.; Liu, Z.; Li, K.; Yang, J.; Qin, G.; Sun, G.; Chen, Q. Tough Interfacial Adhesion of Bilayer Hydrogels with Integrated Shape Memory and Elastic Properties for Controlled Shape Deformation. *ACS Appl. Mater. Interfaces* **2021**, *13*, 10457−10466.
(28) Ju, G.; Cheng, M.; Guo, F.; Zhang, Q.; Shi, F. Elasticity-Dependent Fast Underwater Adhesion Demonstrated by Macroscopic Supramolecular Assembly. *Angew. Chem., Int. Ed. Engl.* **2018**, *57*, 8963−8967.
(29) Ma, C.; Li, T.; Zhao, Q.; Yang, X.; Wu, J.; Luo, Y.; Xie, T. Supramolecular Lego Assembly towards Three-dimensional Multi-responsive Hydrogels. *Adv. Mater.* **2014**, *26*, 5665−5669.
(30) Wu, B.-y.; Xu, Y.-w.; Le, X.-x.; Jian, Y.-k.; Lu, W.; Zhang, J.-w.; Chen, T. Smart Hydrogel Actuators Assembled via Dynamic Boronic Ester Bonds[J]. *Acta Polym. Sin.* **2019**, *50*, 496−504.
(31) Guo, L.; Colby, R. H.; Lusignan, C. P.; Whitesides, T. H. Kinetics of Triple Helix Formation in Semidilute Gelatin Solutions. *Macromolecules* **2003**, *36*, 9999−10008.

https://doi.org/10.1021/acsami.1c21941
ACS Appl. Mater. Interfaces 2022, 14, 3551−3558